Journal of Neuroscience Methods 134 (2004) 81–90

JOURNAL OF NEUROSCIENCE METHODS

www.elsevier.com/locate/jneumeth

High frequency block of selected axons using an implantable microstimulator

Chih-Wei Peng [a], Jia-Jin Jason Chen [a,*], Chou-Ching K. Lin [b], Paul Wai-Fung Poon [c], Chih-Kuo Liang [d], Kang-Ping Lin [e]

[a] Institute of Biomedical Engineering, National Cheng Kung University, 1 University Road, Tainan 701, Taiwan
[b] Department of Neurology, National Cheng Kung University Hospital, Tainan 701, Taiwan
[c] Institute of Physiology, National Cheng Kung University, Tainan, Taiwan
[d] Department of Electrical Engineering, Southern Taiwan University of Technology, Tainan, Taiwan
[e] Department of Electrical Engineering, Chung Yuan Christine University, Chung-Li, and Biomedical Engineering Center, ITRI, Hsinchu, Taiwan

Received 28 May 2003; received in revised form 13 November 2003; accepted 18 November 2003

Abstract

Currently, the majority of neural stimulation studies are limited to acute animal experiments due to lack of suitable implantable microstimulation devices. As an initial step to observe the long-term effects of neural stimulation, a system consisting of an external wireless controller and an implantable dual-channel microcontroller-based microstimulator for tripolar high frequency blocking was developed. The system is not only small in size, and thus suitable for short-term implantation, but also has sufficient current output parameter ranges to meet the demand for high frequency blocking experiments. Using this implantable microstimulator, a series of experiments were conducted on New Zealand rabbit's tibial nerve, including frequency and amplitude selection in driving stimulus and blocking effect tests, which were designed to assess the feasibility and efficiency of the device via torque measurements. Our results showed that the implantable microstimulator system gave a satisfactory performance and could be utilized to achieve selective stimulation and blocking on various sizes of nerve fibers. Our implantable microstimulation system is not only a novel tool for neuromuscular control studies but could also provide a basis for developing various types of sophisticated neural prostheses.

Keywords: Implantable microstimulator; High frequency blocking; Tibial nerve

1. Introduction

Both the sensory and motor nerves in the peripheral nervous system (PNS) are controlled by the central nervous system (CNS). Injuries to the CNS, e.g., spinal cord lesion or stroke, can cause permanent loss of voluntary motor and sensation functions. Electrical activation can restore the deprived motor/sensory functions as long as the peripheral motor and/sensory nerves and muscle below the level of CNS lesion remain intact (Stein et al., 1992). Various types of electrical stimulation techniques have made it possible to restore some motor and sensory functions (Bhadra et al., 2001; Clements et al., 1999; Davis et al., 2001; Loeb et al., 2001).

The development of electrical stimulation systems has moved from surface stimulation (Kralj et al., 1983) and percutaneous stimulation (Scheiner et al., 1994) to a totally implanted stimulation (Bourret et al., 1997). Surface electrical stimulation is used to stimulate the peripheral nerve or muscle by using larger size electrodes attached to the skin surface at some distance from the nerve innervation zone. Generally, surface stimulation is only useful for muscle strengthening but provides less significant functional benefit and lacks selectivity for small muscle groups. In order to obtain a more sophisticated movement or organ function, selective electrical stimulation is applied closely to or directly to the nerve (Fang and Mortimer, 1991; Grill and Mortimer, 1996). Selective stimulation on peripheral nerves is essential for achieving bladder control (Shanker et al., 1998), natural recruitment order for neuroprosthesis control (Solomonow, 1984) and even spasticity suppression (Stefanovska et al., 1988). In addition to spatial selectivity, another important aspect of the electrical stimulation is the fiber diameter selectivity, which refers to the ability to stimulate nerve fibers within a given range of diameters

* Corresponding author. Tel.: +886-6-2757575/63423; fax: +886-6-2343270.
E-mail address: pcw@jason.bme.ncku.edu.tw (J.-J.J. Chen).

0165-0270/$ – see front matter
doi:10.1016/j.jneumeth.2003.11.005

without stimulating those outside that range (Grill and Mortimer, 1995). As the peripheral nerve trunk, the sensory nerve fibers and the motor nerve fibers are intermingled in a complex anatomic layout, it is rather difficult to perform selective stimulation on the peripheral nerve via spatial selectivity and only feasible by modulation of stimulation procedures and parameters (Grill and Mortimer, 1995).

Several nerve selective stimulation procedures, including anodal blocking, collision blocking, and high frequency blocking, have been developed. The anodal blocking technique delivers quasitrapezoidal pulses to the nerve trunk via a symmetric tripolar nerve cuff. As the pulse amplitude increases, action potential may be blocked at the anode (Brindley and Craggs, 1980). However, anodal blocking requires a large amplitude of monophasic current, which might produce irreversible processes at the electrodes and lead to electrode corrosion (Robblee and Rose, 1990). In contrast to the large monophasic stimulus used in anodal blocking, collision blocking utilizes quasitrapezoidal waveforms with an asymmetric tripolar nerve cuff to produce unidirectional action potentials. The action potentials propagate only in the proximal direction from the stimulating electrode, which could collide with action potentials generated by spasticity or other neural muscular stimulation (van den Honert and Mortimer, 1981). The effects of chronic use of the collision blocking technique have demonstrated that repeated action potential generation in the nerve, even at frequencies as low as 50 Hz, can cause early axonal death in less than 8 h. Early axonal death was attributed to the continuous mass activation of the nerves, an essential requirement for collision blocking (Andrews et al., 1990).

Unlike the above two techniques require large amplitudes of monophasic current injection, high frequency blocking inhibits the muscle from contraction just at a suprathreshold level. Therefore, a high frequency blocking technique might be a feasible method for achieving selective stimulation and blocking nerve fibers, which is less likely to cause nerve tissue damage or electrode corrosion in comparison with anodic blocking (Tanner, 1962; McCreery et al., 1990). High frequency blocking techniques for selective stimulation and blocking are based on dual stimuli applied to nerves (Baratta et al., 1989). One stimulus current, called the driving stimulus, is delivered to the proximal site of the nerve trunk, which stimulates nerve fibers of all diameters and produces action potentials. The driving stimulus will produce maximal tetanic muscle contraction while the action potentials are transmitted throughout motor units. Another stimulus current, i.e. the blocking stimulus, is applied to the distal site of the nerve for blocking the action potentials induced by the driving stimulus. By modulating the amplitude of the high frequency current, it could selectively inhibit the action potentials transmitted through out the site.

Previous work has demonstrated that the blocking of axons is dependent on axon size (Tanner, 1962; Baratta et al., 1989). The smaller the axon size, the higher the blocking current amplitude that is needed. Likewise, lower amplitudes can only inhibit larger fibers. Solomonow (1984) indicated that the most effective blocking frequency was around 600 Hz, after testing rectangular monophasic pulses at a range of 600 Hz–20 kHz. A similar blocking technique has been applied to control micturition by inhibiting the contraction of muscle fibers innervated by large diameter axons (Shanker et al., 1998).

However, most of the high frequency blocking studies were restricted to acute animal experiments due to lack of suitable devices that could be implanted in an animal for selective stimulation experiments for a longer period, without re-installation of nerve electrodes while remaining free of infection. Recent advances in microelectronics and micromachining technologies have made it possible to build a small microstimulator for a totally implantable stimulation system. With the implantable microstimulator, the problems of breaking lead wire and infection can be resolved (Loeb et al., 1991, 2001). Nowadays, more and more implantable microstimulation systems have been used to restore damaged or disabled sensory or motor systems (Chervin and Guilleminault, 1994; Eisenberg et al., 1987). Compared to the currently available implantable stimulators, BION implant is a muscle-based microstimulator with capsule-like packaging which is better designed for easy injection and for therapeutic stimulation purpose at a low stimulation rate, no more than 50 pps (Loeb et al., 2001). Other approaches used pacemaker-like implantable stimulator for sacral root stimulation in bladder control, which was generally designed for single-channel selective stimulation with less flexibility in programmable stimulus parameters (Boyer et al., 2000). However, there is paucity of studies that have designed a low cost and small-size wireless-controlled stimulator suitable for high-frequency blocking experiment with special design for dual stimuli nerve (Baratta et al., 1989) applied to axon using nerve cuff electrodes. Before the implantable microstimulator can be considered for long-term application in animals, or even humans, the feasibility and performance must be evaluated. Thus, we first tested the feasibility for an implantable microstimulator system for high frequency blocking, which can perform selective nerve stimulation and blocking of nerve fibers, i.e. recruiting motor units according to their size. A series of animal experiments were designed to assess the performance of the implanted microstimulator device. The ultimate goal is to establish a stimulation technique using the implantable microstimulator as a basis for subsequent long-term evaluation and for various potential clinical applications.

2. Methods and materials

2.1. Implantable microstimulation system

The implantable microstimulation system can be divided into external and implanted modules, as shown in Fig. 1. The

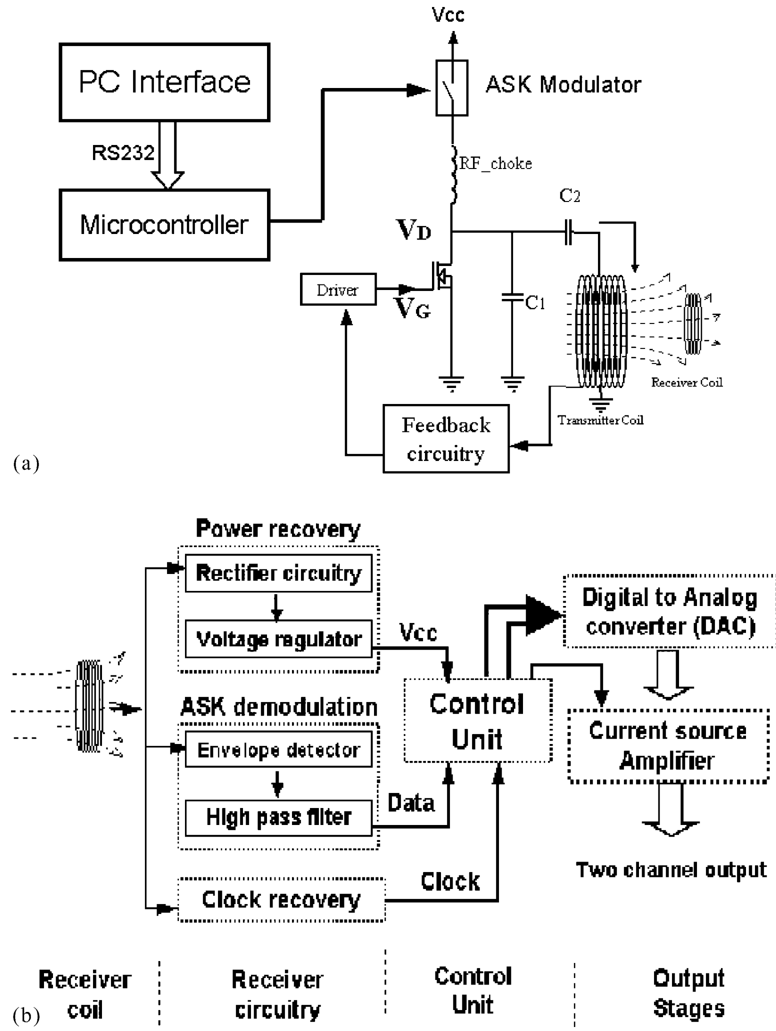

Fig. 1. Schematic representation of (a) the external and (b) the internal implantable microstimulator module.

external module consists of the controller, a radio frequency (RF) transmitter, and a transmitting coil. Digital data and command are encoded and streamed in a series of pulses, which are sent to the high efficiency RF transmitter and are inductively coupled to the implanted module. As shown in Fig. 1(a), the transmitted RF electromagnetic wave is picked up by receiver coil of the implanted module, which is further rectified and regulated as the sole energy source for the microstimulator system. Meanwhile, the modulated RF signal is demodulated and sent to the internal digital controller for data decoding, stimulation patterns generation and channel selection. According to the received data, the microstimulator generates the predefined stimulation waveforms that are conducted to nerve cuff electrode for selective nerve stimulation and blocking purpose.

A detailed block diagram of the external module is depicted in Fig. 1(b). After the selection of stimulation parameters, the data are arranged into a defined format for two separated channels and are encoded for further RF modulation and wireless transmission. In the wireless transmission for the implanted module, both power and data are transcutaneously transmitted, using the inductive coupling between the transmitter coil and the receiver coil. Among the various power amplifiers, the class E amplifier has highly efficient properties when transmitting RF power via an inductive coupling and is capable of supplying sufficient power to the implantable microstimulator for operation (Zierhofer and Hochmair, 1990). The inductive coupling is similar to a transformer that uses a magnetic flux link, but without a conducting ferrite core. In choosing the RF carrier frequency, one should consider the trade-off between transmission rate and tissue absorption. In this study, we chose a carrier frequency of 2 MHz, which is adequate for transmission with minimal tissue absorption.

In order to maximize the inductive transcutaneous link for an implant, several factors, including coupling efficiency, displacement tolerance, and communication bandwidth should be considered. Various approaches have been proposed to maximize power transfer efficiency and displacement tolerance, and to widen the communication bandwidth which need the proper matching and setup of the transmitting and receiving coil circuits (Heetderks, 1988;

Zierhofer, 1996). However, efficiency and displacement tolerance are opposing tradeoffs (Heetderks, 1988). One of the general approaches is to design a special geometric coupling coil in an attempt to keep the coupling coefficient constant by using a larger primary coil, or enhancing the coupling coefficient by distributing the turns of the coils across the radii (Zierhofer, 1996). However, a smaller power receiver coil is generally required in miniaturized implants. This limits the increase of the power transfer by prohibiting simple enlargement of the transmitting coil. In addition to coil geometrical design, other approaches have employed a higher efficiency amplifier in the transcutaneous transmitters (Zierhofer and Hochmair, 1990). The class E amplifier, using a self-oscillating technique was adopted herein for the realization of a high efficiency power/data inductive link (Zierhofer and Hochmair, 1990).

Apart from an efficient inductive coupling, well-designed external and internal controllers are essential for providing a high degree of programmability and flexibility in control procedures or experiments. The major considerations include precise external control of stimulation parameters, simple and user-friendly external controllers, small size and good encapsulation, high reliability, and long lifetime. Our implantable system has two independent stimulation channels. One is designed for stimulation experiments that require low stimulation frequency with monophasic pulses. The other is aimed at high frequency blocking experiments in which a train of monophasic pulses with a higher frequency is desired. The stimulation parameters can be set up from the external controller and sent in single data transmissions for various stimulation frequencies, durations, and intensities. Once the parameters have been set, there is no need to send them again unless a new stimulation pattern is required. However, power transmission requires the continuous transfer of RF power to the implant in order to provide a stable power supply.

2.2. Animal surgery

High frequency blocking experiments were conducted on 15 male New Zealand white rabbits between 2.0 and 3.0 kg. All animals were anaesthetized with ketamine hydrochloride via intravenous injection on the ear (3 mg/kg/min, i.v.). The hair over lateral side of thigh was removed before operating the rabbit. A sterile technique was used to incise on the lateral side of the right hindleg from midthigh to popliteal fossa and the tibial nerve was exposed. After sterilization, animals were applied with an implanted microstimulation system module, which was hermetically packaged and implanted within the subcutaneous tissue over the lateral side of the hindleg. Meanwhile, a self-coiling spiral tripolar nerve cuff electrodes, 20 mm in length and 6 mm between rings, for dual stimuli was applied to the tibial nerve (Baratta et al., 1989). After surgical implantation, the animal was returned to its cage and properly treated to prevent wound inflammation. The animal was given at least 3 days to recover from the surgical operation and the first experiment was performed 3–7 days after the implantation. During the experiment, the animals were continuously injected ketamine hydrochloride to maintain deep anesthesia. All experimental procedures used in this study complied with the National Cheng Kung University Hospital Regulations for animal use and care.

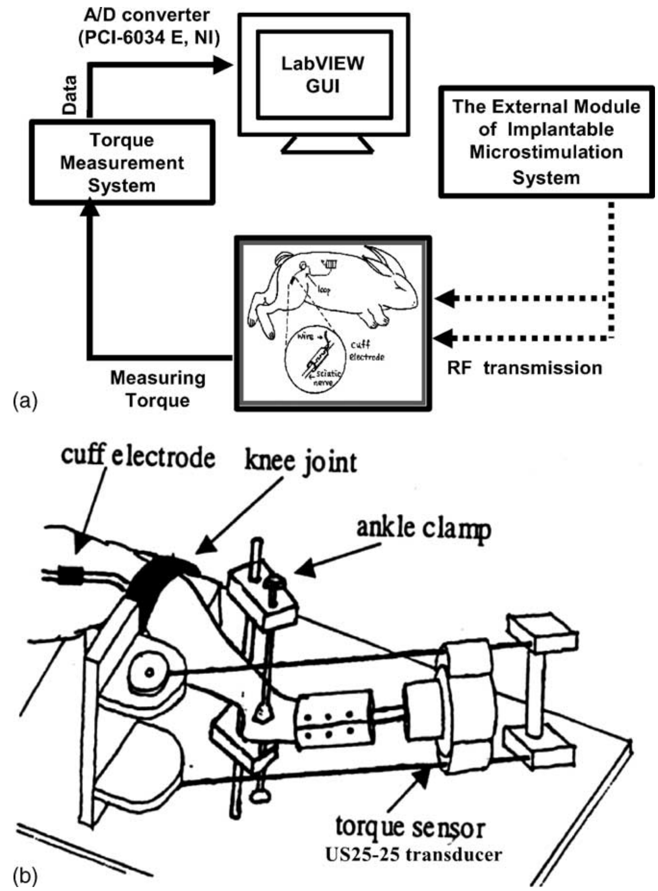

Fig. 2. (a) Animal experimental setup used for measuring the isometric reactive torque and (b) during selective stimulation studies.

2.3. Experimental procedure

The flowchart of the entire experimental system is shown in Fig. 2. The external implantable microstimulation system module was utilized to modulate the microstimulation system that was implanted within the rabbit's hindlimb, producing two channels of stimulus currents via an RF transmission. Since the tibial nerve innervates the rabbit's calf muscle, the magnitude of ankle joint torque produced from the calf muscle should be proportional to the activation level of the tibial nerve. Therefore, by analyzing the changes of torque, it is possible to measure the effect of the selective stimulation of the microstimulator system. In our study, the torque measurement system was designed to measure the three-dimensional (3D) isometric torque generated at the rabbit ankle joint under the various stimulus parameters applied to the tibial nerve. The system was built around a commercially available 3D force and movement transducer (US25-25, ATI, USA) on a platform. A fixture was designed to interface the sensor with the rabbit's hindlimb. The fixture can be adjusted to a suitable position in order to clamp the knee and foot of various sizes of rabbits, as shown in Fig. 2(b). The animal was mounted in the measurement platform with hip, knee, and ankle joint set about to 80°, 85°, and 100°, respectively. In this study, the ankle joint will obviously produce plantar–flexion torque as the tibial nerve is stimulated. Compared to torque measured in plantar–flexion direction, torque measured in other directions are rather small that can be neglected. Thus, only the plantar–flexion torque axis was selected as an index for assessing the performance of the electrical nerve stimulation and blocking. The changes of isometric torque under the various stimuli modulations were measured and stored on a computer for further analysis via an A/D converter (PCI-6034E, NI Corp., sampling rate of 100 Hz).

Generally, three major stimulation parameters, i.e. stimulation intensity, pulse width (PW), and frequency can be used to modulate the muscle force output. A series of experiments were first performed to establish suitable parameters for the driving stimulus of selective nerve stimulation, including the stimulation frequency and maximal stimulation intensity for each animal. To determine the desirable stimulation frequency, we first fixed the pulse width and amplitude at 100 μs and 0.26 mA, respectively, with a monophasic waveform. Under these stimulation conditions, we recorded the isometric torque response under various pulse frequencies (20–80 Hz) for a second driving stimulus. The stimulation frequency, which can generate smooth and tetanic muscle contraction, was chosen for the driving stimulus. With the selected stimulation frequency and fixed stimulation width (at 100 μs), the next experiment was designed to determine the threshold value for the smallest motor nerve fibers by measuring the nerve recruitment curve. The recruitment curve measured the recruited muscle force, in terms of the reactive torque versus the applied stimulation amplitudes for a period of 1 s. We could thus find the maximal tetanic torque stimulation amplitude from the recruitment curve that can be utilized in subsequent nerve blocking experiments.

To observe the blocking effect, we delivered a driving stimulus using the selected stimulation parameters to produce tetanic contraction for a period of 5 s. During this driving stimulus duration, we simultaneously applied a blocking stimulus to reduce the tetanic torque to between 1 and 3 s. The blocking effect under various blocking current intensities can be evaluated by calculating the ratio of the maximal amount of torque which was blocked ($T_m - T_b$) as compared with the initial average maximal tetanic contraction (T_m), as formulated in the following equation:

$$\text{Blocking effect} = \frac{T_m - T_b}{T_m} \times 100\%$$

where T_m, average maximal available torque before blocking; and T_b, residual torque after a 2 s blocking period.

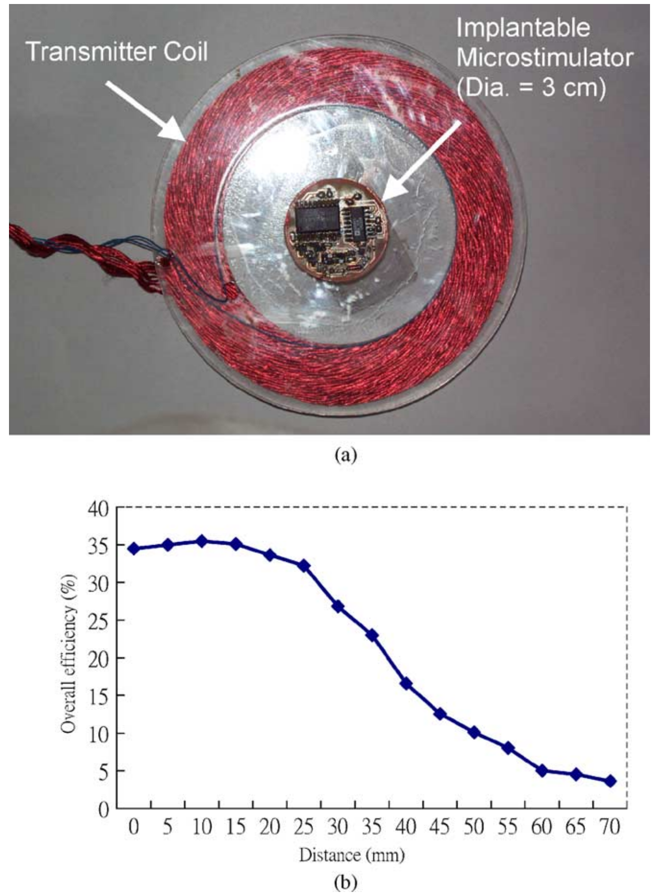

Fig. 3. (a) Photograph of the implantable microstimulator before casting, and of the transmitter coil and (b) the overall efficiency vs. the coupling distance between the external transmitter and implanted microstimulator.

3. Results

3.1. Implementation of an implantable microstimulation system

Fig. 3(a) shows the size and configuration of the RF transmission coil and a two-channel implantable microstimulator system before casting, which was designed and fabricated for high frequency blocking animal experiments. The size of the RF transmitter coil (9 cm for the o.d. and 7 cm for the i.d.) is larger than the implanted module (3 cm in diameter), so that the misalignment of the implanted module is more tolerable. The transmitter coil is made of Litz wire (strands 48 AWG) formed in multi-twisted thin lines with eight bundles in a line and 175 strands in a bundle, giving a high inductance value for the same cross-sectional area (21 μH with 13 turns).

The quality (Q) value of our transmitter can reach up to 470, which consumes less power with better coupling efficiency. However, too high a Q value might cause oversensitivity, in the coupled RF signal, to a lateral or longitudinal displacement between the transmitter and receiver coils. The implantable microstimulation system is fabricated mostly with surface mount device (SMD) components and mounted on a double-layer printed circuit board (PCB) with a 3 cm diameter. The receiver coil is also made of Litz wire (strands 48 AWG of 13 turns) and is arranged in a ring around the outline of the PCB with an inductance of 7.4 μH and a Q value of 63. The overall efficiency of the RF power transmission scheme is defined as the ratio of the power delivered to the load of the implanted system and the overall dc-power consumption of the external transmission system. With good tuning at the switching point, the self-oscillating class E power amplifier has very high power transmission efficiency, usually above 90%. Thus, the coupling distance becomes the major power loss source during wireless transmission, and the key factor influencing power efficiency. Fig. 3(b) shows the overall efficiency versus the coupling distance. The power coupling efficiency decreases significantly with the increase of the coupling distance, especially at more than 35 mm. In our current setup, the maximum stimulus current output can reach 1 mA when the load impedance is at 1 kΩ. This current intensity is sufficient for most neural stimulation and blocking applications. The overall power dissipation of the implanted system is around 30 mW. Low power consumption is an essential design criterion, especially for an implanted device without an internal battery. The detailed specifications and the components are listed in Table 1.

3.2. Stimulation procedures for driving stimulus

Usually the stimulation frequency is one of the key electrical parameters affecting the smoothness of muscle contraction. Fig. 4(a) shows the isometric torque in plantar–flexion direction in one stimulation case under different stimulation frequencies, ranging from 20 to 80 Hz, with a monophasic rectangular waveform fixed at 100 μs and 0.26 mA. A suitable frequency is determined, by which a fused and smooth contraction can be achieved. We can observe that the torque continually increases with the increase of frequency. Meanwhile, the coefficient of variance (CV) which measures the variation of torque during the stimulation duration, decreases from 90.84 to 13.09% as the stimulation frequency increases from 20 to 50 Hz. The CV obtained from experiments in five rabbits reaches a plateau and fluctuates below around 10% when the stimulation frequency is at a high level, between 60 and 80 Hz, as shown in Fig. 4(b). We can observe that a higher stimulation frequency, above 60 Hz, can provide a smoother torque output.

After identifying the stimulation frequency required to produce a smooth torque, we needed to further determine the stimulation intensity for generating a tetanic contraction. In order to produce tetanic contractions, the maximal recruitment level should be determined first. The recruitment characteristics of a rabbit's tibial nerve was tested under various stimulation current amplitudes, starting at 0.02 mA with an increment of 0.02 mA. The stimulus pulse was set as a monophasic pulse with a duration of 100 μs at a fixed stimulation frequency of 60 Hz. Fig. 5 shows the data from a normalized isometric recruitment curve obtained from one rabbit, which appears to be of a sigmoid shape, and will finally reach a plateau level even if the current amplitude is continuously increased. Therefore, the recruitment curve shown in Fig. 5 reveals that the threshold for achieving maximal tetanic contraction is at least greater than 0.3 mA.

3.3. Effect of blocking stimulation

After the selection of a suitable stimulation frequency and amplitude for producing smooth and tetanic torque, a 600 Hz monophasic blocking waveform was used to modulate recruitment torque. As determined in the previous section, the driving stimulus was fixed at 60 Hz with a 100 μs pulse width. The stimulation intensity needed to generate the maximal recruitment torque was determined before each blocking test.

Fig. 6(a) shows representative patterns of torque measurements before and during application of various amplitudes of the 600 Hz monophasic rectangular blocking stimulus. The muscle force maintained a relatively stable torque output during the first second of the initial driving stimulation. The addition of a 600 Hz blocking stimulus to the tibial nerve did not cause a sudden drop in torque, but showed a slow decline during the blocking stimulus. After cessation of the blocking stimulus, the background tetanic torque rapidly returned, though occasionally not entirely, to the original level. During the blocking period, some small residual torque always remained in all trials. It seems that a transient increase in torque obviously appeared when a higher blocking stimulus was applied.

The blocking effects with respect to the various blocking current amplitudes of a 600 Hz monophasic rectangular waveform are summarized in Fig. 6(b). At lower blocking currents, the blocking effect was not evident (10% at

Table 1
Microstimulator specifications and components

Components	Contents
Receiver coil	Litz wire, AWG 48, 30 mm diameter, $L = 7.4\,\mu$H, $Q = 63$
Transmitter coil	Litz wire, 80 mm diameter, 12 turns $L = 21\,\mu$H
Power amplifier	Class E amplifier
Carrier frequency	2 MHz
Modulation and encoding	Amplitude shift keying modulation with pulse width coding
Data rate	20 kbps
Internal voltage rectifier	3 V for analogue and 4.5 V for digital
Stimulation channels	One for nerve stimulation and one for nerve blocking
Stimulation pulse-frequency	10 ∼ 90 Hz, 100 ∼ 900 Hz with 16 selections
Stimulation pulse-width	100 ∼ 900 μs, divided into 16 steps
Stimulation pulse-amplitude	0.02 ∼ 1 mA, 64 steps 0.02 ∼ 1 mA, 64 steps
PCB material	Glass-epoxy double sided

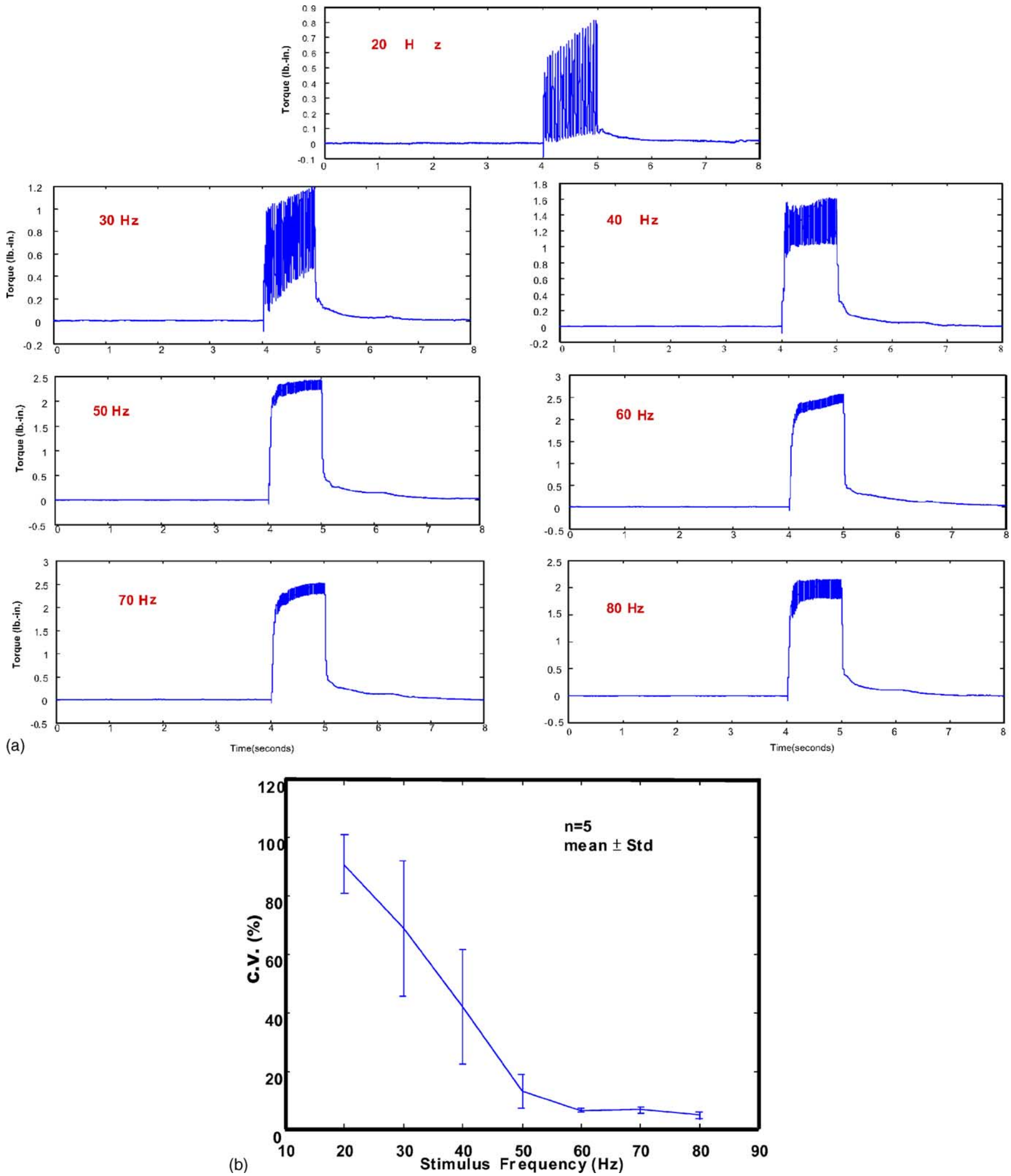

Fig. 4. (a) Example of the isometric torque that was recorded at various frequencies of the driving stimulus. The coefficient of variance (CV) obtained from five rabbits and (b) is used to measure the smoothness of muscle contraction for various stimulation frequencies. Smoother reactive torque, e.g. CV below 10%, can be found when the stimulation frequency is above 60 Hz.

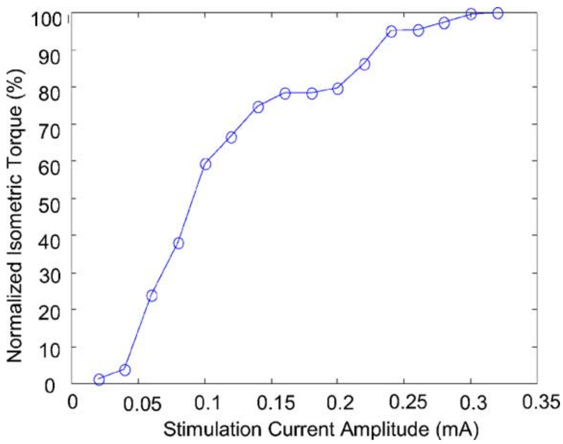

Fig. 5. A sigmoid-like normalized reactive torque obtained at various stimulation intensities can be used to estimate the maximal driving stimulus.

0.25 mA blocking intensity). After that, the blocking effect increases gradually until a maximum limit is reached (93.2% blocking effect at 0.8 mA in this case). After reaching the maximum, the blocking effect remained relatively constant, even where using higher blocking current amplitudes (Fig. 6(b)).

4. Discussion and conclusion

We have successfully implemented a wireless implantable microstimulator by using SMD components. This prototype of an implantable microstimulator system is built on a double layer PCB with a 3 cm diameter, and the overall power consumption of the implanted device is around 30 mW. This system excludes many of the problems often encountered in implantable devices, such as infection caused by electrode leads that pierce the skin, or surgery necessary to replace an implanted battery. The portable design of the external controller provides flexibility for animal experiments or for future clinical applications in a patient's daily life. The RF receiver front-end of the implanted unit has two voltage regulators that provide power for both the digital and analog circuits. Our results indicate that the system output can perform at stable stimulation and power level when the two coils are within a 30 mm range. The designed prototype microstimulator has been used for short-term animal experiments with an initial sealing package. The hermetical sealing of the implant is essential to ensure that body fluids do not leak into, and thus cause the malfunction of the implanted device. The design principles and experience gathered from establishing the wireless power/data transmission in this work can serve as a basis for future application-specific integrated circuit design.

Under the present stimulation procedures of driving stimulus, our results suggest that a suitable stimulation frequency for generating a smoother torque output, with minor variation, ranged from 60 to 80 Hz. However, Solomonow et al. (1983) studies showed that a stimulation frequency of 30–70 Hz could provide smooth and useful contraction. Previously, it had been demonstrated that a higher stimulation frequency, above 45–50 Hz tends to cause rapid fatigue of the muscle and consequent deterioration of its force level. In contrast, we imposed a more restrictive criterion with a variance of generated torque below 10%. Our selection of 60 Hz for the stimulation frequency was based on this criterion and was used throughout the entire animal experiment. The discrepancies in the suitable stimulation frequency range could be due to the different animals used in these studies, i.e. cats, where we used New Zealand rabbits. For any neuroprostheses applied in clinical trials, muscle fatigue is a critical factor. Thus, a muscle fatigue test must be an important part of evaluating the feasibility of an implantable microstimulator in any future clinical application. With regard to the drive stimulus current amplitude, a sigmoid recruitment curve shape was measured in our study, as observed by other investigators (Gorman and Mortimer, 1983). Clearly, the threshold may be changed in other studies due to different animal, electrode type, stimulation waveform and duration of implantation. It is suggested that an isometric recruitment curve be obtained before each selective stimulation and blocking experiment.

With regard to the blocking stimulation effects, our results in Fig. 6 showed that the blocking effect gradually increased with the increase of blocking intensity, which permitted a finely modulated control. Although some minimum residual torque always existed, about 8% of the maximal tetanic torque, the blocking stimulus could attenuate almost 90% of the reactive torque. This phenomenon closely resembled that obtained by Solomonow (1984). Moreover, others have demonstrated that the same blocking scheme could selectively recruit muscle motor units from small to large while the blocking intensity is gradually decreased from the maximal blocking situation (Baratta et al., 1989). Therefore, we have indirectly demonstrated the effect of selective stimulation on the size of the nerve fibers. This stimulation scheme could compensate the drawback of conventional neural stimulation methods which can only recruit muscle nerves in a reverse order compared to the physiologic manner (Blair and Erlanger, 1933). With the implantable microstimulator and a high-frequency blocking scheme, we can therefore perform axon stimulation in a natural recruitment order for varied in-vivo animal studies, such as muscle fatigue via electrical stimulation.

Presently, we have established the high frequency blocking technique and achieved finely modulated control with the implanted device under short-term implantation. The developed microstimulator is capable of providing a miniaturized implantable device for performing dual-channel stimulation and blocking experiments. Our future studies will focus on encapsulating the entire internal module with a biocompatible material, thus aiming to long-term chronic implantation. In addition, a bi-directional transmission technique is also under development, which not only can transmit data from

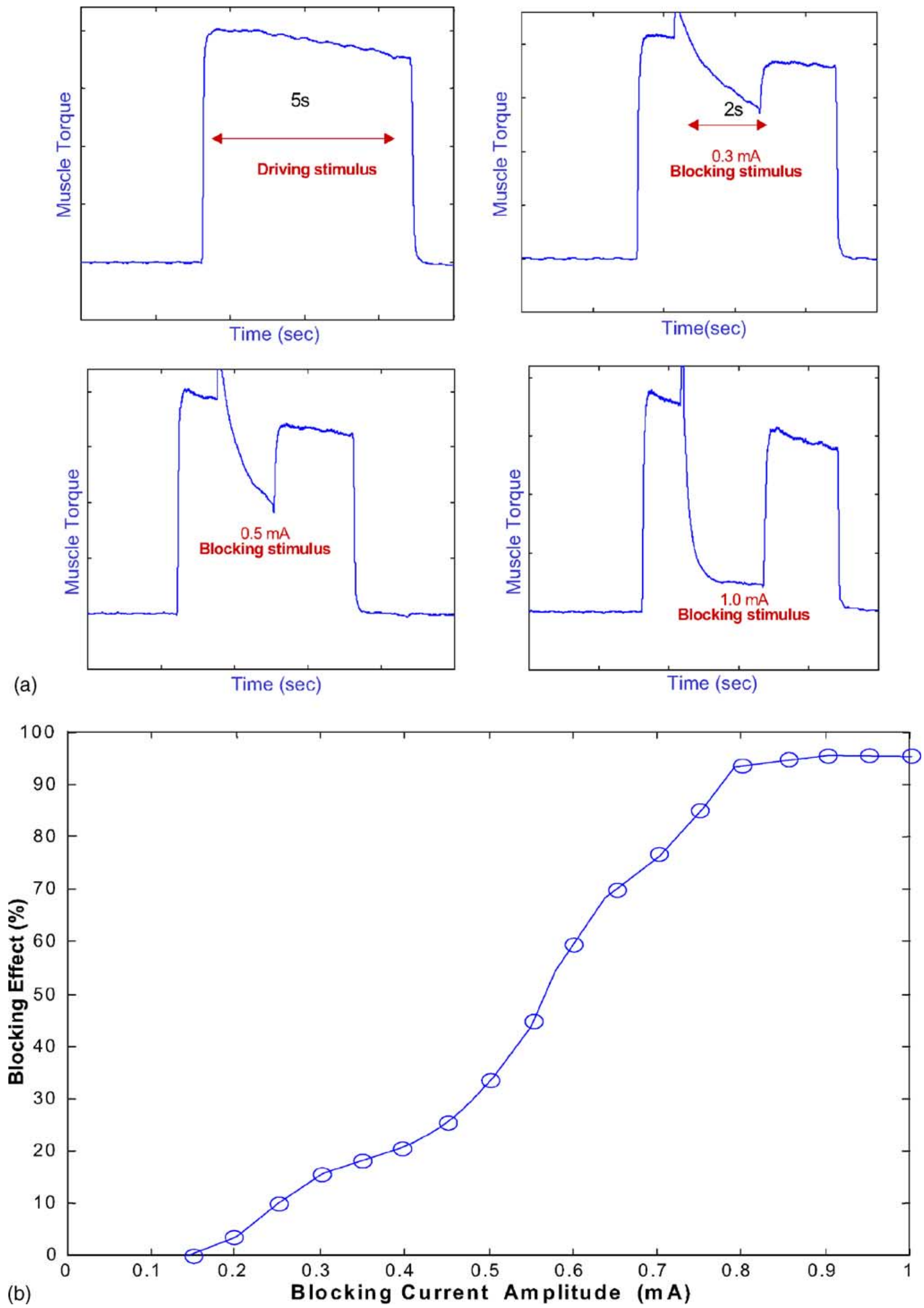

Fig. 6. Typical examples of blocking effects performed on New Zealand rabbits using the implantable microstimulator. (a) During 5 s of driving stimulation, the torque attenuated while applying various levels of blocking stimulus ranging from 0 to 1.0 mA and (b) the blocking effect of various blocking intensities.

the external module but also send the acquired physiological signal outwards. With a bi-directional communication scheme and miniature sensing or stimulating device, many novel medical microdevices can be employed for in-vivo measurement or treatment. The microstimulation controller architecture proposed in this study is highly versatile and can be easily modified for other types of implantable neural prostheses or medical devices. This new technology has the potential to become a viable alternative for rehabilitation in neurological disorders.

Acknowledgements

This work was partially supported by the National Health Research Institute, Taiwan, ROC, under grants

NHRI-EX91-9017EP and by the Ministry of Education, Taiwan, ROC, under grants 89-B-FA08-1-4.

References

Andrews WF, McCreery DB, Bullara LA, Yuen TGH. Effects of prolonged electrical stimulation of peripheral nerve. Neural Prostheses: Fundamental studies. New Jersey: Prentice Hall; 1990.

Baratta R, Ichue M, Hwang SK, Solomonow M. Orderly stimulation of skeletal muscle motor units with tripolar nerve cuff electrode. IEEE Trans Biomed Eng 1989;36:836–43.

Blair E, Erlanger J. A comparison of the characteristics of axons through their individual electrical responses. Am J Physiol 1933;6:524–64.

Bhadra N, Kilgore KL, Peckham PH. Implanted stimulators for restoration of function in spinal cord injury. Med Eng Phys 2001;23:19–28.

Bourret S, Sawan M, Plamondon R. Programmable high-amplitude balanced stimulus current-source for implantable microstimulators. Proc IEEE Int Eng Med Biol Soc 1997;5:1938–41.

Boyer S, Sawan M, Abdel-Gawad M, Robin S, Elhilali MM. Implantable selective stimulator to improve bladder voiding: design and chronic experiments in dogs. IEEE Trans Rehabil Eng 2000;8:464–70.

Brindley GS, Craggs MD. A technique for anodally blocking large nerve fibers through chronically implanted electrodes. J Neurol Neurosurg Psychiatry 1980;43:1083–90.

Chervin RD, Guilleminault C. Diaphragm pacing: review and reassessment. Sleep 1994;17:176–87.

Clements M, Vichiechom K, Hughes C, Liu W, McGucken E, Demarco C, Mueller J, Humayun M, de Juan E. An implantable neuro-stimulator device for a retinal prosthesis. San Francisco: ISSCC; 1999. p. 15–17.

Davis R, Patrick J, Barriskill A. Development of functional electrical stimulators utilizing cochlear implant technology. Med Eng Phys 2001;23:61–8.

Eisenberg LS, Maltan AA, Portillo JP, Mobley JP, House WF. Electrical stimulation of auditory brainstem in deafened adults. J Rehabil Res Dev 1987;24:9–22.

Fang ZP, Mortimer JT. Selective activation of small motor axons by quasitrapezoidal current pulses. IEEE Trans Biomed Eng 1991;38:168–74.

Gorman PH, Mortimer JT. The effect of stimulus parameters on the recruitment characteristics of direct nerve stimulation. IEEE Trans Biomed Eng 1983;30:407–14.

Grill WM, Mortimer JT. Stimulus waveforms for selective neural stimulation. IEEE Trans Biomed Eng 1995;42:168–74.

Grill WM, Mortimer JT. Non-invasive measurement of the input-output properties of peripheral nerve stimulating electrodes. J Neurosci Methods 1996;65:43–50.

Heetderks WJ. RF Powering of millimeter and submillimeter sized neural prosthetic implants. IEEE Trans Biomed Eng 1988;35:323–7.

Kralj A, Bajd T, Turk R, Krajnik J, Benko H. Gait restoration in paraplegic patients: a feasibility demonstration using multichannel surface electrode FES. J Rehabil Res Dev 1983;20:3–20.

Loeb GE, Peck RA, Moore WH, Hood K. BION^{TM} system for distributed neural prosthetic interfaces. Med Eng Phys 2001;23:9–18.

Loeb GE, Zamin CJ, Schulman JH, Troyk PR. Injectable microstimulator for functional electrical stimulation. IEEE Trans Biomed Eng Comput 1991;29:13–9.

McCreery DB, Agnew WF, Yuen TGH, Bullara LA. Charge density and charge per phase as cofactors in the induction of neural injury by electrical stimulation. IEEE Trans Biomed Eng 1990;37:996–1001.

Robblee LS, Rose TL. Electrochemical guidelines for selection of protocols and electrode materials for neural stimulation. Neural prostheses: Fundamental studies. New Jersey: Prentice Hall; 1990.

Scheiner A, Polando G, Marsolais EB. Design and clinical application of a double helix electrode for functional electrical stimulation. IEEE Trans Biomed Eng 1994;41:425–31.

Shanker HS, Tu LM, Robin S, Arabi K, Hassouna M, Sawan M, Elhilali MM. Reduction of bladder outlet resistance by selective sacral root stimulation using high-frequency blockade in dogs: an acute study. J Urol 1998;160:901–7.

Solomonow M, Eldred E, Lyman J, Foster J. Fatigue considerations of muscle force during high frequency stimulation. Am J Phys Med 1983;62:117–22.

Solomonow M. External control of the neuromuscular system. IEEE Trans Biomed Eng 1984;31:752–63.

Stefanovska A, Gros N, Vodovnik L. Chronic electrical stimulation for the modification of spasticity in hemiplegic patients. Scand J Rehabil Med Suppl 1988;17:115–21.

Stein RB, Peckham PH, Popovic DB. Neural prostheses: replacing motor function after disease or disability. New York: Oxford University Press; 1992.

Tanner J. Reversible blocking of nerve conduction by alternating current excitation. Nature 1962;195:712–3.

van den Honert C, Mortimer JT. A technique for collision block of peripheral nerve: Single stimulus analysis. IEEE Trans Biomed Eng 1981;28:373–8.

Zierhofer CM. Geometric approach for coupling enhancement of magnetically coupled coils. IEEE Trans Biomed Eng 1996;43:708–14.

Zierhofer CM, Hochmair ES. High-efficiency coupling-insensitive transcutaneous power and data transmission via an inductive link. IEEE Trans Biomed Eng 1990;37:716–22.